

Light-Patterned Crystallographic Direction of a Self-Organized 3D Soft Photonic Crystal

Zhi-Gang Zheng, Cong-Long Yuan, Wei Hu, Hari Krishna Bisoyi, Ming-Jie Tang, Zhen Liu, Pei-Zhi Sun, Wei-Qiang Yang, Xiao-Qian Wang, Dong Shen, Yannian Li, Fangfu Ye, Yan-Qing Lu,* Guoqiang Li,* and Quan Li*

Uniform and patterned orientation of a crystallographic direction of ordered materials is of fundamental significance and of great interest for electronic and photonic applications. However, such orientation control is generally complicated and challenging with regard to inorganic and organic crystalline materials due to the occurrence of uncontrollable dislocations or defects. Achieving uniform lattice orientation in frustrated liquid-crystalline phases, like cubic blue phases, is a formidable task. Taming and tailoring the ordering of such soft, cubic lattices along predetermined or desired directions, and even imparting a prescribed pattern on lattice orientation, are more challenging, due to the entropy-domination attribute of soft matter. Herein, we disclose a facile way to realize designed micropatterning of a crystallographic direction of a soft, cubic liquid-crystal superstructure, exhibiting an alternate uniform and random orientation of the lattice crystallographic direction enabled by a photoalignment technique. Because of the rewritable trait of the photoalignment film, the pattern can be erased and rewritten on-demand by light. Such an oriented soft lattice sensitively responds to various external stimuli such as temperature, electric field, and light irradiation. Furthermore, advanced reflective photonic applications are achieved based on the patterned crystallographic orientation of the cubic blue phase, soft lattice.

photons.^[1] The inherent molecular self-organization capability of soft matter embodies prominent advantages compared to the common microprocessing and nanoprocessing techniques, such as photolithography, electron-beam lithography, and etching, from the viewpoint of fabrication.^[2] Liquid crystals (LCs) are representative stimuli-responsive soft matter with excellent self-organized behavior. LC phase displaying 3D cubic architectures (i.e., blue phases, BPs) with lattice-constant dimensions of hundreds of nanometers, determined by helical pitch, exhibits versatile and promising photonic properties.^[3] BPs, which are commonly observed between the isotropic phase and chiral nematic (otherwise referred to as cholesteric, N*) phase in strong chiral systems, possess cubic structures built by double-twisted cylinders formed by LC molecules, according to the Oseen–Frank elastic model.^[4] Such a delicate, 3D, cubic nanostructure endows BP with exotic optical isotropy and significant selective photonic reflection of circularly polarized light, having the same handedness with the BP helix.^[5] The central wavelength of the reflection band, in the case of normal incidence, can be determined as $\lambda = \frac{2na}{\sqrt{h^2 + k^2 + l^2}}$ for

3D photonic superstructures are widely investigated and are remarkable owing to their complex and peculiar structures, which readily enables manipulation of the flow of light or

ized light, having the same handedness with the BP helix.^[5] The central wavelength of the reflection band, in the case of normal incidence, can be determined as $\lambda = \frac{2na}{\sqrt{h^2 + k^2 + l^2}}$ for

Prof. Z.-G. Zheng, C.-L. Yuan, Z. Liu, P.-Z. Sun, W.-Q. Yang,
Dr. X.-Q. Wang, Prof. D. Shen
Department of Physics
East China University of Science and Technology
Shanghai 200237, China

Prof. Z.-G. Zheng, Dr. H. K. Bisoyi, Dr. Y. Li, Prof. Q. Li
Liquid Crystal Institute and Chemical Physics Interdisciplinary Program
Kent State University
Kent, OH 44242, USA
E-mail: qli1@kent.edu

Prof. W. Hu, M.-J. Tang, Prof. Y.-Q. Lu
National Laboratory of Solid State Microstructures
Collaborative Innovation Center of Advanced Microstructures
and College of Engineering and Applied Sciences
Nanjing University
Nanjing 210093, China
E-mail: yqlu@nju.edu.cn

Prof. F. Ye
Beijing National Laboratory for Condensed Matter Physics
and CAS Key Laboratory of Soft Matter Physics
Institute of Physics
Chinese Academy of Sciences
Beijing 100190, China

Prof. G. Li
Visual and Biomedical Optics Lab
Department of Ophthalmology and Visual Science
and Department of Electrical and Computer Engineering
Ohio State University
Columbus, OH 43212, USA
E-mail: li.3090@osu.edu

DOI: 10.1002/adma.201703165

a BP with lattice constant, a , and crystallographic direction, $[h\ k\ l]$; h , k , and l are Miller indices. Herein, n is the average refractive index of a blue phase liquid crystal (BPLC). In the past decade, many studies have been devoted to clarify the phase structure of BP, both theoretically and experimentally.^[6] Moreover, soft matter features of BPs render them responsive to external stimuli, such as temperature,^[7] electric field,^[8] and light,^[9] resulting in tunable performance of BP-based photonic devices.

From the processing viewpoint of BP devices, alignment-free is well-known and regarded as one of the most prominent advantages of such devices, which yields a colorful mosaic platelet texture due to the random distribution of the crystallographic direction of BP domains. Nevertheless, some recent reports, achieving a narrower reflection-band width, stronger reflectance, and better electro-optical performances, have indicated the occurrence of a uniform crystallographic direction of BP, enabled by treatment of substrate surfaces for homogeneous alignment.^[10] Dramatic reduction of pumping energy for laser emission was found in an aligned BPLC.^[10c] Preliminary investigations on light reflectance and phase after impinging on aligned BPLC have also been carried out.^[10d] Moreover, the mechanism for the formation and orientation uniformity of BP lattices in such a surface-alignment case has been explained via nucleation kinetics^[11] and a Kössel diagram.^[12]

A uniform orientation, and even the micropatterning of a crystallographic direction to a prescribed structure without a conspicuous orientation defect of the lattice, are desired and of great interest in electronic and photonic applications.^[13] However, such a task is generally complicated and challenging with regard to inorganic materials, such as graphene, and even more difficult in case of organic materials. Recently, a very weak effect on the orientation of BP lattices was noticed when a BP system containing an azo dye was irradiated with light. However, the photoinduced preferred orientation of BP lattices was neither uniform nor stable.^[14] Herein, we disclose a facile way to realize micropatterning of a crystallographic direction of the soft cubic BP superstructure, exhibiting alternate uniform and random orientation of the lattice crystallographic direction with high resolution, enabled by photoalignment treatment of the substrates through a judiciously designed photomask. Furthermore, such a superstructure can be deformed and recovered by applying and removing external stimuli, such as temperature and electric field, owing to the soft and dynamic attributes of BPLC. Although the patterning of organic crystals used as an electronic transistor array was reported through printing with a surface-relief polydimethylsiloxane stamp,^[13a] the well-defined fusion/conglomeration of uniform and random lattice orientations through such a noncontact and one-time processing photoalignment with stimuli-responsiveness has not been demonstrated, to the best of our knowledge. Distinct from previously reported methods to generate the uniformity of a lattice crystallographic direction,^[13] the alternate patterns obtained herein can be erased and rewritten readily by a combination of electric field and light stimulus. Reflective diffraction devices based on different designed patterns have been developed. These alternating patterns could be promising for application in advanced reflective photonic systems that are important for spectral analysis and imaging.^[15]

An empty LC cell with the substrates coated with a photoalignment layer (Figure S1, Supporting Information) on the inner surface was irradiated by a linearly polarized UV beam through a square-patterned binary photomask (Figure 1a). The newly fabricated LC mixture exhibiting BP (phase sequence: Iso 55.0 °C BP 51.5 °C N*) was filled into the cell at isotropic temperature and slowly cooled. A patterned crystallographic direction of a cubic BP lattice was achieved, exhibiting a periodic alternating crystallographic orientation, i.e., uniform at the exposed areas and random at the unexposed areas (Figure 1b). The regularly distributed squares, exhibiting uniform and identical reflection color under polarized optical microscope (POM) in reflection mode (Figure 1c) indicate a uniform BP lattice orientation promoted by surface homogeneous alignment at the exposed areas. This observation strongly suggests that uniformly oriented islands of BP lattices have been selectively achieved in the sea of an unaligned BP sample by a patterned UV irradiation. To further corroborate the uniformity of the crystallographic orientation and distinguish such orientation of the aligned and unaligned areas, we carried out investigations by comparing the Kössel diffraction diagrams in the corresponding areas. Figure 1d(i) shows a conspicuous circular ring observed in the UV exposed areas at 53.5 °C. Such a diagram was recorded and compared from twenty different regions in each exposed area and between the different exposed areas, and no significant difference was found when the sample temperature was maintained, which shows the uniformity of crystallographic orientation of the aligned BP lattice at the exposed squares; whereas, the Kössel diagram in an unexposed area does not yield such a sharp pattern with regular shape, rather a pattern with many obscure curves overlapped together (Figure 1d(ii)) due to the random orientation and small domain-size of the BP lattice in this region. It was found that a uniform lattice orientation of the BP lattice over large exposed areas, as well as tiny feature sizes with a scale down to $\approx 12\ \mu\text{m}$ without any conspicuous orientation defects, can be achieved by similar technique according to the optical textures and Kössel diagram (Figure S2(i)–(v),(viii), Supporting Information), which demonstrates that a uniform orientation of such a soft lattice can be obtained conveniently by photoalignment technique, both on microscopic and macroscopic scales, therefore indicating a powerful capability of such a technique for achieving uniform crystallographic orientation of a BP soft lattice. The satisfactory patterns of uniform crystallographic orientation can also be obtained in a cell if the patterned photoalignment treatment was performed on only one substrate (Figure S2(vi),(vii), Supporting Information). The clear characters can also be recorded in cells with photoalignment treatment on one substrate (Figure S2(ix),(x), Supporting Information). Besides, varying photoalignment direction on one substrate with respect to the other substrate, but maintaining the thickness of the cell, does not affect the occurrence of uniform lattice orientation of the BP (Figure S3a,b, Supporting Information); the orientation uniformity is unchanged due to the statistically isotropic arrangement of LCs. However, the uniformity of the alignment quality drops in the case of a large cell gap, such as $12\ \mu\text{m}$ (Figure S3c, Supporting Information). Therefore, it is possible to achieve uniform lattice orientation of the BP soft lattice, not only in homogeneous cells, but also in hybrid treated cells containing a photoalignment layer by a remote-controlled physical method.

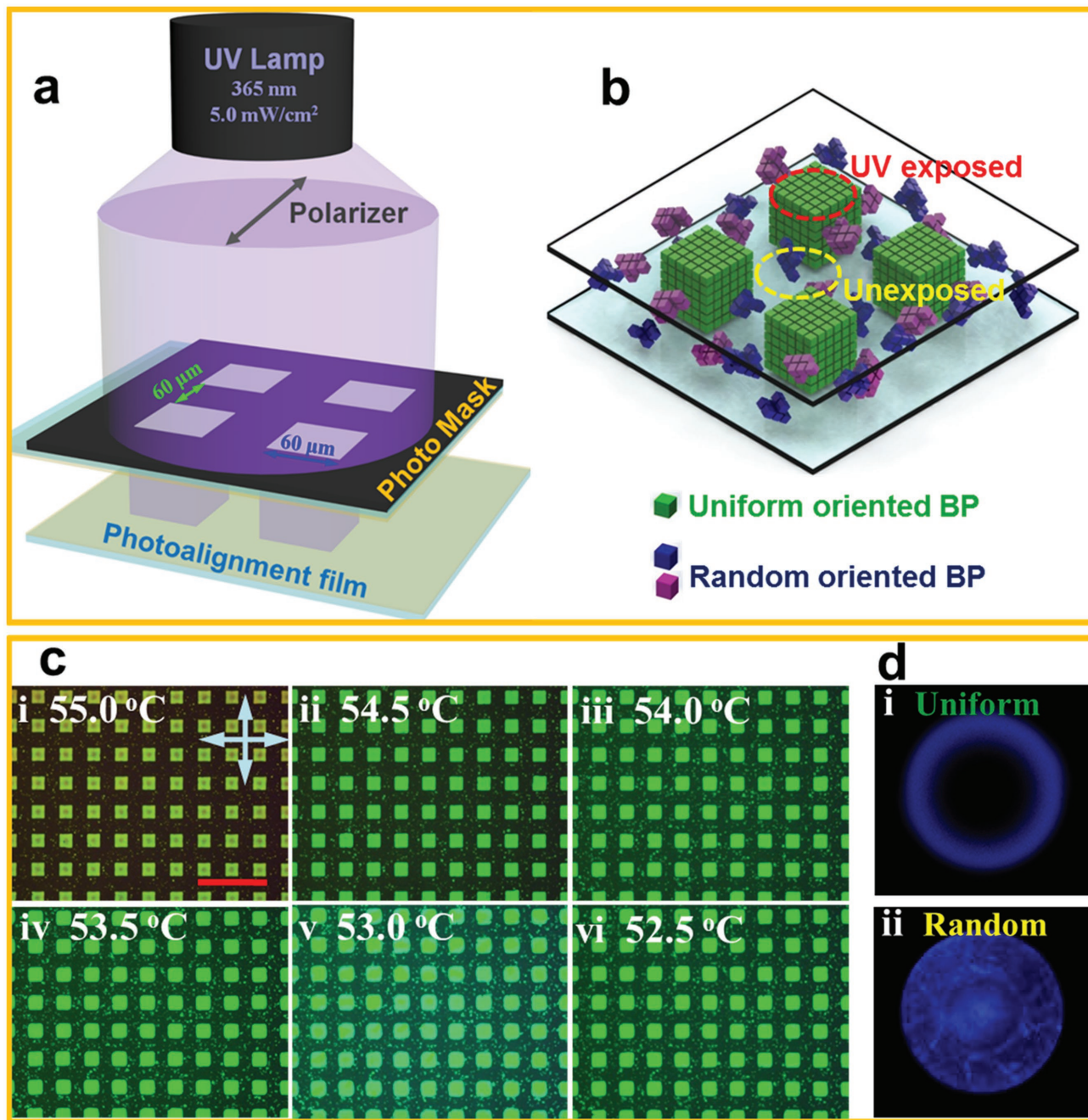


Figure 1. Uniform and random crystallographic orientation pattern of BP soft lattice realized by photoalignment. a) Cell fabrication. The empty cell coated with photoalignment film on the inner surfaces of two substrates was exposed by a collimated linearly polarized UV light through a binary photomask with square pattern (square size: $60 \times 60 \mu\text{m}^2$). Therefore, the photoalignment agent promotes homogeneous alignment in the exposed areas and no preferred alignment in the unexposed areas. b) Schematic diagram about the distribution of cubic BP lattice. The green cube represents the uniform oriented BP lattices, while the blue and purple cubes represent the randomly oriented BP lattice. The aligned areas are full of uniform cubic BP with a green color, exhibiting a regularly stratified structure. In nonaligned areas, cubic BP crystallites are randomly oriented dispersed in the cell, with no preferred crystallographic orientations. c) Typical POM textures of a thermally tunable BP lattice pattern observed under reflection mode with crossed polarizers (orthogonal double-arrows). The bright square regions are photoaligned BP with uniform lattice orientation, while the comparatively dark regions are nonaligned BP with random orientations. The scale bar is $300 \mu\text{m}$. All the POMs were recorded with a cooling rate at $0.3 \text{ }^\circ\text{C min}^{-1}$. d) Kössel diagrams recorded in photoaligned and unaligned areas detected at the same temperature, $53.5 \text{ }^\circ\text{C}$. i) The circular ring pattern indicates a uniform orientation of BP lattice. ii) The unaligned area showed Kössel diffraction pattern with overlapped, irregular, and obscure curves.

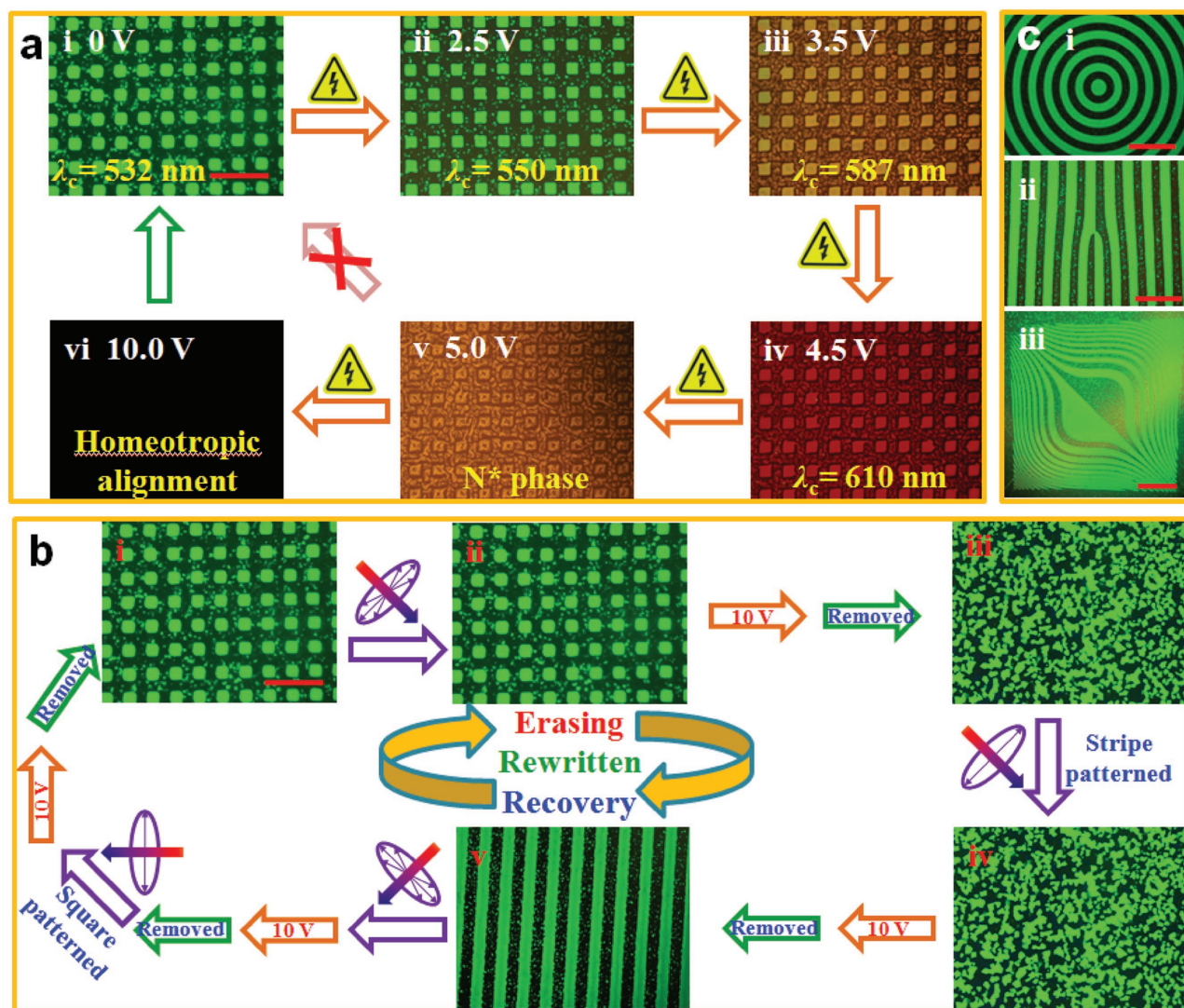


Figure 2. Stimuli-directed behavior of the crystallographic orientation pattern formed by alternate uniform and random BP domains. a) The BP lattice can be deformed by an applied voltage, leading to a red-shifting of the central wavelength of reflection band from i) the initial 532 nm in no-bias state, passing through ii) 550 nm and iii) 587 nm, driven respectively by 2.5 and 3.5 V voltages, to iv) 610 nm as such voltage reaches 4.5 V; v) further enhancement of the voltage to 5.0 V induces a phase transition to N* phase, which can not revert back to the initiation BP after removing the voltage; vi) a continual increment of the voltage to 10.0 V leads to the helix unwinding and homeotropic alignment of LC molecules, presenting a dark state which, however, can recover to the initial state after removing the voltage. b) The pattern can be erased and rewritten by sequential UV-irradiation and electric-field stimulation. i,ii) The initial periodic square pattern cannot be erased even after undergoing an irradiation of unpolarized UV light solely; iii) such pattern is erased by applying and removing a 10.0 V applied voltage after the exposure by a unpolarized UV light, forming a random oriented BP; iv) this random oriented BP is still maintained even after exposed by a linear polarized UV light passing through a stripe binary photomask before applying and removing the voltage; v) the straight stripe pattern appears after applying and removing a 10.0 V applied voltage; similarly, such stripe pattern can recover to the initial square pattern via the same aforementioned way. c) Another different regular periodic patterns and irregular topological patterns can be rewritten, such as the i) concentric circular pattern; ii) stripe with a “fork” shaped dislocation at the center; iii) complicated topological pattern for generating Airy beam. The experimental temperature is maintained at 53.5 °C. The scale bars in the figure represent 300 μm.

A prominent feature of such an alternate uniform and random orientation pattern formed by the BP lattice is its responsiveness, on demand, with respect to various external stimulations due to its soft attribute, which is not available to common organic and inorganic crystalline materials. As the sample was cooled from 55.0 to 52.5 °C, the reflective color of uniform oriented BP lattice changed from yellowish green, passing through green, partial bluish green, and finally back to green (Figure 1c). The corresponding reflective spectra exhibited

a blue-shift from 573 nm at 55.0 °C to 527 nm at 53.0 °C, followed by a red-shift to 543 nm (Figure S4a, Supporting Information), confirming the texture observation. Furthermore, on applying an electric-stimulus at 53.5 °C, the reflective color responded fast, changing from green with the central reflection wavelength of 532 nm in case of 0 V bias to red with the central reflection wavelength of 610 nm when applying a 4.5 V (Figure 2a). Continuous increase of the voltage to 5.0 V led to an electric-field-induced phase transition from BP to N* phase,

showing a significant widening of spectral band-width as well as a weakening of reflectance due to light scattering in N^* phase (Figure S4b, Supporting Information). Another unusual observation is that the BP did not recover to the original BP pattern but maintain at N^* phase, as the 5.0 V was removed. Whereas, if the voltage was increased to 10.0 V to induce a helix unwound resulting in homeotropic alignment of LC molecules and then removed, the BP with the original lattice orientation pattern reappeared (Figure 2a(i),(v),(vi)), indicating a bistability of the pattern. Such surface alignment can be erased under an unpolarized UV light irradiation (5.0 mW cm^{-2}), however the most distinct aspect herein is that such uniform and random orientation of BP lattice, exhibiting a 2D periodic square pattern, was maintained after such irradiation (Figure 2b(ii)), rather than getting destroyed as usually occurs in photoaligned nematic LC. However, it is interesting to note that a random orientation of BP lattice formed as a 10.0 V field was applied and removed quickly (Figure 2b(iii)). Subsequently, the sample was exposed to a polarized UV light (5.0 mW cm^{-2}) through a binary stripe photomask for about 16 min, followed by applying and removing a 10.0 V voltage, the original 2D square pattern of oriented BP was erased and transformed to the 1D stripe pattern, corresponding to the photomask (Figure 2b(v)). The stripe pattern can recover to the original square pattern with a following pattern-erasing by the combined effects of unpolarized UV and electric-field, and pattern-recovery by the combination of square-patterned polarized UV exposure and electric-field stimulation (Figure 2b(v),(i)). Another regular or irregular topological pattern can be rewritten with the combination effects of light and electric-field, such as a concentric circle (Figure 2c(i)), a stripe pattern with embedded “fork” dislocation at the central region of the pattern, the so called fork grating (Figure 2c(ii)) and a very complicated pattern (Figure 2c(iii)) which is promising for application as an Airy beam generator.

Such periodic square patterns formed by the alternate uniform and random oriented BP lattice exhibit interesting optical diffraction at the reflection side as a right-handed circular polarized light (RCPL), which has the same handedness with the BP helix, impinged perpendicular to the sample. The reflected diffraction beams were turned by a beam splitter and received by a black screen (the experimental setup is shown in Figure 3a). When the external bias was absent at the initiation, the corresponding central reflection wavelength of the reflection band at square areas was $\approx 532 \text{ nm}$ (Figure 3c), inducing a 2D diffraction array in the case of a light incidence by 532 nm RCPL (Figure 3b(i)), however no diffraction appeared if the wavelength of RCPL was moved out of such reflection band, for instance, 650 nm (Figure 3b(ii)). By applying an external bias of 3.5 V on the sample shifted the reflection band to the central wavelength of 587 nm, thereby leading to the disappearance of diffraction corresponding to 532 nm RCPL (Figure 3b(iii)), whereas, interestingly, a similar 2D diffraction exhibited in the situation of an incidence of 589 nm RCPL (Figure 3b(iv)). Such light diffraction was caused by the strong contrast of reflection intensity between the uniform and random oriented BP areas with respect to the impinged RCPL having the wavelength included into the reflection band (Figure 3c), which means that light diffraction occurred selectively to certain wavelengths, i.e., wavelength-selectivity. Notably, the missing of even diffraction

orders, for instance, $\pm 2\text{nd}$ -order, was evident, independent of the wavelength of RCPL, due to such binary change on the reflection intensity (see the Supporting Information). Although the wavelength-selective diffraction based on light stimulated photoresponsive cholesteric LC has been achieved in our recent work,^[16] the performance obtained by electric-field directed BPLC has not been reported to the best of our knowledge. Notably, an advantage of BPLC is the narrower reflection band compared with cholesteric system, which improves the wavelength-sensitivity of the diffraction.

Fork grating (FG) is known as a convenient photonic device to generate optical vortices,^[17] which provides broad applications in diverse areas of micromanipulation,^[18] telecommunications,^[19] and quantum-information.^[20] The optical vortex is characterized by corkscrew wave front and a donut-like intensity distribution along its axis of propagation. Herein, the number of phase windings in a single wavelength around the axis is called the topological charge m , and the donut-like intensity distribution is determined by the topological charge as well. The diffraction of FG was investigated through the same experimental setup shown in Figure 3a. When a 532 nm RCPL impinges to FG, diffraction beams with optical vortex, whose topological charge increases along with diffraction order, inducing gradual expansions of the low-intensity central dark region and the surrounding high-intensity ring, were received at the black screen, i.e., reflection side (Figure 3d(i)). Further intensity distribution analysis of the 1st and 2nd diffraction orders (Figure 3d(ii),(iii)) showed well consistency with the observation in the experiment. From the perspective of applications, since photoalignment agent is an optically sensitive material, the optical stability of these devices is essential for long-term applications. It was found that the morphology of such patterns could be retained almost invariable for at least 6 h (Figure S5(i)–(iv), Supporting Information) when irradiated by a 532 nm RCPL with the intensity of 5.5 mW cm^{-2} . When a 10.0 V voltage was applied and removed on the sample, such morphology was still maintained (Figure S5(v), Supporting Information). Such result also confirms the optical stability and robustness of different patterns formed with the distribution of uniform and random oriented BP domains. Besides, all the properties of such uniform and random oriented BP pattern, for instance, temperature and electric-field induced shifting of reflection band, are retained in FG. Thus, the FG demonstrated herein is a reflective and wavelength-selective device, which is distinct from the earlier reported cases. In view of further convenient applications, a wider temperature range of BP with preferable responsiveness to external stimulations is always favorable, such as the BPLC composed of bimesogens^[5] and the BPLC doped with appropriate amount of bent-core materials.^[21] Herein, the commonly used polymer-stabilized BPLC formed by UV-light irradiation is not a suitable candidate, due to the influence of alignment direction caused by UV-light. Although the manner to reinforce such alignment direction has been developed,^[22] the rewritability of photoalignment film is sacrificed.

In conclusion, we have demonstrated that cautiously designed alternate uniform and random orientations of the crystallographic direction of BP soft lattice with high resolution can be fabricated by means of a photoalignment

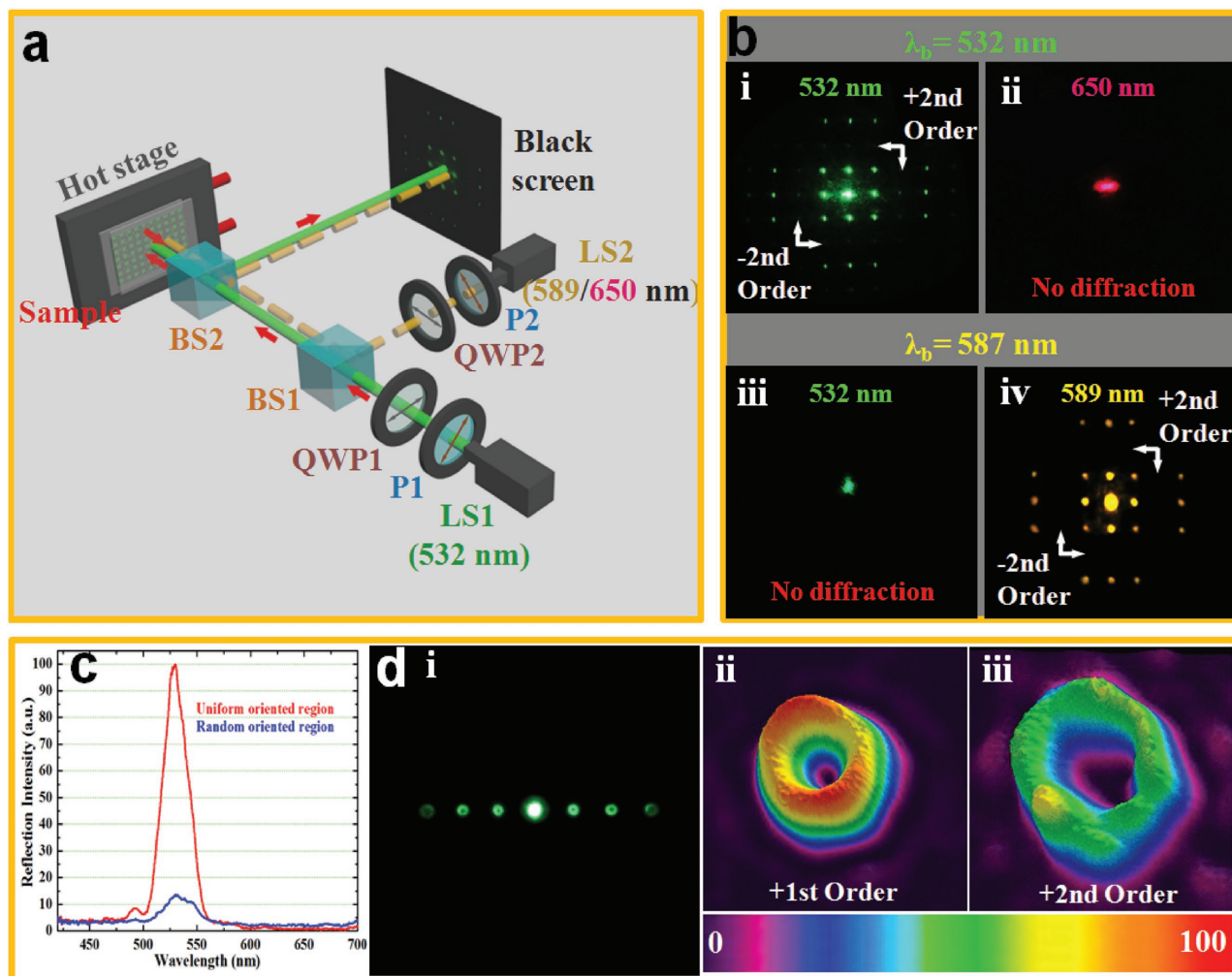


Figure 3. Photonic applications of the crystallographic orientation pattern formed by alternate uniform and random BP domains. a) Optical setup of diffraction detection. The 532 nm laser light (LS1) is converted to RCPL after successively passing through a polarizer (P1) and a quarter waveplate (QWP1); the angle between the transmission axis of polarizer and the fast axis of quarter waveplate is 45° . The RCPL impinges on the sample by passing through two beam splitters (BS1 and BS2), generating the diffraction. The diffractive light was turned by BS2, which is placed very close to the sample, and was projected on a black screen. The short red arrows show the propagation direction of the beam. As the wavelength of testing source is changed to 589 or 650 nm, the LS1 is turned off, while the other laser source (LS2) is turned on; the light path is turned by BS1 and BS2 and overlapped with that of 532 nm laser after the light is converted to RCPL. b) At the initial state without applied bias, the central wavelength of reflection band, λ_b , is 532 nm, leading to a) 2D diffraction pattern; however ii) no diffraction is observed when the impinging wavelength is 650 nm. The central wavelength of reflection band is red-shifted to 587 nm after applying 3.5 V, which induces a iii) disappearance of diffraction with respect to 532 nm laser, while replaced by iv) an appearance of diffraction to the yellow-colored 589 nm laser. The even diffraction orders, such as ± 2 nd order as labeled in figures (i) and (iv), are missed, i.e., missing order. c) The reflection spectra of uniform (red curve) and random (blue curve) oriented BP regions. The reflection intensity of aligned areas is about 6 times higher than that of the nonaligned areas. d) The diffraction pattern of Fork grating shown in Figure 2c(ii). i) Diffraction pattern received on black screen, similar as the diffraction pattern of common 1D grating, but with a small dark dot in the center of every diffraction order. The donut-shaped intensity distributions of ii) +1st and iii) +2nd orders are detected and analyzed by charge-coupled device (CCD) beam profiler. The color bar represents the intensity from the lowest (violet) to the highest (red). The experiment is carried out at 53.5°C .

technique. Furthermore, one of the remarkable advantages of the technique resulting in uniformly oriented islands in a sea of a randomly oriented matrix of cubic BP thin film is photorewritability. Such a superstructure can be arbitrarily erased and reconfigured to other periodic or topological patterns with high resolution. Based on the soft attribute of BP, the patterned superstructure can respond to temperature and electric field leading to stimuli-directed changes on optical properties, such as reflection intensity, reflection band, and light scattering, and is promising to be adopted in advanced reflective optical

and photonic devices. This work could broaden the application scope of BPLC and could provide some guidelines toward the controllability of crystallographic orientation of other soft organic and inorganic materials, where orientation control is critical for their functionality and performance.

Experimental Section

Materials: BP was obtained through composition of 96.4 wt% commercial eutectic nematic LC host (TEB300, supplied by Slichem,

China) and 3.6 wt% chiral dopant (R5011, supplied by HCCH, China). Herein, a sulfonic azo dye (SD1, synthesized in the lab), whose chemical structure is shown in Figure S1 (Supporting Information), was an appropriate choice to be used as the photoalignment agent considering the better alignment stability, stronger surface anchoring, higher resolution, and more robust rewritability, compared with other photoalignment materials employed in the literature.^[23]

Cell Fabrication: Two indium-tin-oxide-coated glass slices were used as the cell substrates. The glass substrates were water-bathed under ultrasonic wave and illumination-cleaned by UV-Ozone. Then, the photoalignment agent SD1, which was dissolved in *N,N*-dimethylformamide with a concentration of 1.0 wt%, was spin-coated on the substrates with a strong adhesion to ensure the uniformity of the alignment layer. Finally, two substrates were assembled together and sealed by epoxy glue, while the cell gap was maintained by 5.0 μm spacers.

Photoalignment Implementation: The UV-light generated from a mercury lamp (SunSpot 2, Uvitron), precisely collimated by a group of lenses, passed through a nanowire-grid polarizer, and then normally irradiated through a binary photomask, which was in close contact with the prepared cell for an exposure dose of about 5.0 mW cm^{-2} for 16 min. As the SD1 molecules undergo an exposure of a polarized UV light, the molecules will tend to reorient their absorption oscillators perpendicular to the polarization of the UV light, subsequently guiding LC directors to realign along the direction of SD1, i.e., perpendicular to polarization direction of UV, through intermolecular interactions. Such alignment direction of LC molecules can be reoriented by rotating the polarization direction of the UV light.^[24] Thereafter, the LC mixture was injected into the cell by capillarity at isotropic phase.

Characterization: BP texture was observed by the polarized optical microscopy (LVPOL 100, Nikon) while the temperature was precisely controlled by a hot stage (HCS302, Instec). The samples were heated to the isotropic state at 70 $^{\circ}\text{C}$ and then slowly cooled to BP at a rate of 0.3 $^{\circ}\text{C min}^{-1}$ and maintained at 53.5 $^{\circ}\text{C}$ for testing. POMs were recorded by a digital camera (DS-U3, Nikon) and the reflectance spectra were recorded by a fiber connected spectrometer (ULS2048, Avantes). Generally, the uniformity of crystallographic orientation of lattice is corroborated through X-ray diffraction due to the nanometer or sub-nanometer dimensions of the common inorganic crystal. Herein, the visible light was used as the light source to detect the diffraction caused by the cubic BP structure with the lattice constant of several hundreds of nanometers, i.e., the Kössel diffraction method, which is well adopted in the orientation investigation of BPLC in widespread.^[12] A monochromatic laser was employed as the light source; and the corresponding Kössel diagrams were received at the back focal plane of a high numerical aperture (NA) oil immersed objective ($\times 100/\text{NA} = 1.25$, oil, Plan, Nikon). The electrically induced color shift was studied by applying a 1 kHz alternating current square wave across the sample. The laser sources with output wavelengths of 532, 589, and 650 nm were used to detect the waveband-selective diffraction. The intensity distribution of the optical vortices was detected and simultaneously analyzed by a CCD beam profiler system (SP620U, Spiricon).

Supporting Information

Supporting Information is available from the Wiley Online Library or from the author.

Acknowledgements

Z.-G.Z., C.-L.Y., and W.H. contributed equally to this work. The authors acknowledge the support from the National Key Research and Development Program of China (2017YFA0303700), the Ohio Third Frontier, the National Science Foundation of China (Grant Nos. 61435008 and 61575063), Shanghai Rising-Star Program (Grant No. 17QA1401100), the National Institutes of Health (through National

Eye Institute, Grant No. R01EY020641), and State of Ohio TVSF fund (through Grant No. TCEG201604).

Conflict of Interest

The authors declare no conflict of interest.

Keywords

3D photonic crystals, crystallographic directions, photoalignment, self-organized cubic superstructures, stimuli-responsive

Received: June 6, 2017

Revised: July 13, 2017

Published online: August 28, 2017

- [1] a) S. Noda, K. Tomoda, N. Yamamoto, A. Chutinan, *Science* **2000**, 289, 604; b) N. Liu, H. Guo, L. Fu, S. Kaiser, H. Schweizer, H. Giessen, *Nat. Mater.* **2008**, 7, 31.
- [2] a) Y. N. Xia, B. Gates, Z. Y. Li, *Adv. Mater.* **2001**, 13, 409; b) M. Campbell, D. N. Sharp, M. T. Harrison, R. G. Denning, A. J. Turberfield, *Nature* **2000**, 404, 53; c) H. K. Bisoyi, Q. Li, *Acc. Chem. Res.* **2014**, 47, 3184.
- [3] a) L. Wang, Q. Li, *Adv. Funct. Mater.* **2016**, 26, 10; b) H. K. Bisoyi, Q. Li, *Chem. Rev.* **2016**, 116, 15089.
- [4] S. Meiboom, M. Sammon, W. F. Brinkman, *Phys. Rev. A* **1983**, 27, 438.
- [5] H. J. Coles, M. N. Pivnenko, *Nature* **2005**, 436, 997.
- [6] a) H. Delacroix, J. M. Gilli, I. I. Erk, P. Mariani, *Phys. Rev. Lett.* **1992**, 69, 2935; b) K. Higashiguchi, K. Yasui, H. Kikuchi, *J. Am. Chem. Soc.* **2008**, 130, 6326; c) T. Shu, Y. Hiroyuki, K. Yuto, K. Ryusuke, N. Ryuji, O. Masanori, *Sci. Rep.* **2015**, 5, 16180.
- [7] S. T. Hur, B. R. Lee, M. J. Gim, K. W. Park, M. H. Song, S. W. Choi, *Adv. Mater.* **2013**, 25, 3002.
- [8] C. W. Chen, C. C. Li, H. C. Jau, L. C. Yu, C. L. Hong, D. Y. Guo, C. T. Wang, T. H. Lin, *ACS Photonics* **2015**, 2, 1524.
- [9] T. H. Lin, Y. Li, C. T. Wang, H. C. Jau, C. W. Chen, C. C. Li, H. K. Bisoyi, T. J. Bunning, Q. Li, *Adv. Mater.* **2013**, 25, 5050.
- [10] a) P. Nayek, H. Jeong, H. R. Park, S. W. Kang, S. H. Lee, H. S. Park, H. J. Lee, H. S. Kim, *Appl. Phys. Express* **2012**, 5, 051701; b) J. Yan, S. T. Wu, K. L. Cheng, J. W. Shiu, *Appl. Phys. Lett.* **2013**, 102, 011113; c) K. Kim, S. T. Hur, S. Kim, S. Y. Jo, B. R. Lee, M. H. Song, S. W. Choi, *J. Mater. Chem. C* **2015**, 3, 5383; d) H. Yoshida, J. Kobashi, *Liq. Cryst.* **2016**, 43, 1909.
- [11] a) P. J. Chen, M. Chen, S. Y. Ni, H. S. Chen, Y. H. Lin, *Opt. Mater. Express* **2016**, 6, 1003; b) O. Henrich, K. Stratford, D. Marenduzzo, M. E. Cates, *Proc. Natl. Acad. Sci. USA* **2010**, 107, 13212.
- [12] a) R. J. Miller, H. F. Gleeson, *J. Phys. B: At. Mol. Phys.* **1996**, 6, 909; b) P. Nayek, N. H. Park, S. C. Noh, S. H. Lee, H. S. Park, H. J. Lee, C. T. Hou, T. H. Lin, H. Yokoyama, *Liq. Cryst.* **2015**, 42, 1111; c) E. Oton, E. Netter, T. Nakano, D. K. Y. F. Inoue, *Sci. Rep.* **2017**, 7, 44575.
- [13] a) A. L. Briseno, S. C. Mannsfeld, M. M. Ling, S. Liu, R. J. Tseng, C. Reese, M. E. Roberts, Y. Yang, F. Wudl, Z. Bao, *Nature* **2006**, 444, 913; b) A. E. Espinal, L. Zhang, C. H. Chen, A. Morey, Y. Nie, L. Espinal, B. O. Wells, R. Joesten, M. Aindow, S. L. Suib, *Nat. Mater.* **2010**, 9, 54; c) Y. Hao, M. S. Bharathi, L. Wang, Y. Liu, H. Chen, S. Nie, X. Wang, H. Chou, C. Tan, B. Fallahzad, H. Ramnarayan, C. W. Magnuson, E. Tutuc, B. I. Yakobson, K. F. McCarty, Y. W. Zhang, P. Kim, J. Hone, L. Colombo, R. S. Ruoff, *Science* **2013**, 342, 720; d) W. Yang, G. Chen, Z. Shi, C. C. Liu, L. Zhang, G. Xie,

- M. Cheng, D. Wang, R. Yang, D. Shi, K. Watanabe, T. Taniguchi, Y. Yao, Y. Zhang, G. Zhang, *Nat. Mater.* **2013**, *12*, 792.
- [14] a) C. R. Lee, T. L. Fu, K. T. Cheng, T. S. Mo, A. Y. G. Fuh, *Phys. Rev. E* **2004**, *69*, 031704; b) D. Fedorenko, K. Slyusarenko, E. Ouskova, V. Reshetnyak, K. Ha, R. Karapinar, Y. Reznikov, *Phys. Rev. E* **2008**, *77*, 061705; c) H. Y. Liu, C. T. Wang, C. Y. Hsu, T. H. Lin, *Appl. Opt.* **2011**, *50*, 1606; d) A. Y. G. Fuh, S. T. Wu, T. H. Lin, Y. Zhou, Y. Huang, *Opt. Express* **2006**, *14*, 4479.
- [15] J. W. den Herder, A. C. Brinkman, S. M. Kahn, G. Branduardi-Raymont, K. Thomsen, H. Aarts, M. Audard, J. V. Bixler, A. J. den Boggende, J. Cottam, T. Decker, L. Dubbeldam, C. Erd, H. Goulooze, M. Güdel, P. Guttridge, C. J. Hailey, K. Al Janabi, J. S. Kaastra, P. A. J. de Korte, B. J. van Leeuwen, C. Mauche, A. J. McCalden, R. Mewe, A. Naber, F. B. Paerels, J. R. Peterson, A. P. Rasmussen, K. Rees, I. Sakelliou, M. Sako, J. Spodek, M. Stern, T. Tamura, J. Tandy, C. P. de Vries, S. Welch, A. Zehnder, *Astron. Astrophys.* **2001**, *365*, L7.
- [16] P. Z. Sun, Z. Liu, W. Wang, L. L. Ma, D. Shen, W. Hu, Y. Q. Lu, L. J. Chen, Z. G. Zheng, *J. Mater. Chem. C* **2016**, *4*, 9325.
- [17] a) B. Y. Wei, W. Hu, Y. Ming, F. Xu, S. Rubin, J. G. Wang, V. Chigrinov, Y. Q. Lu, *Adv. Mater.* **2014**, *26*, 1590; b) X. W. Xu, D. Luo, H. T. Dai, *IEEE Photonics J.* **2016**, *8*, 1.
- [18] Y. Zhao, J. S. Edgar, G. D. Jeffries, D. McGloin, D. T. Chiu, *Phys. Rev. Lett.* **2007**, *99*, 073901.
- [19] J. Wang, J. Y. Yang, I. M. Fazal, N. Ahmed, Y. Yan, H. Huang, Y. X. Ren, Y. Yue, S. Dolinar, M. Tur, A. E. Willner, *Nat. Photonics* **2012**, *6*, 488.
- [20] G. Molina-Terriza, J. P. Torres, L. Torner, *Nat. Phys.* **2007**, *3*, 305.
- [21] a) W. Q. Yang, G. Q. Cai, Z. Liu, X. Q. Wang, W. Feng, Y. Feng, D. Shen, Z. Zheng, *J. Mater. Chem. C* **2017**, *5*, 690; b) H. Wang, Z. Zheng, D. Shen, *Liq. Cryst.* **2012**, *39*, 99.
- [22] Q. Guo, A. K. Srivastava, V. G. Chigrinov, H. S. Kwok, *Liq. Cryst.* **2014**, *41*, 1465.
- [23] a) V. Chigrinov, E. Prudnikova, V. Kozenkov, H. Kwok, H. Akiyama, T. Kawara, H. Takada, H. Takatsu, *Liq. Cryst.* **2002**, *29*, 1321; b) X. Zhao, A. Bermak, F. Boussaid, T. Du, V. G. Chigrinov, *Opt. Lett.* **2009**, *34*, 3619; c) P. Chen, B. Y. Wei, W. Ji, S. J. Ge, W. Hu, F. Xu, V. Chigrinov, Y. Q. Lu, *Photonics Res.* **2015**, *3*, 133; d) A. Muravsky, A. Murauski, V. Chigrinov, H. S. Kwok, *J. Soc. Inf. Disp.* **2008**, *16*, 927.
- [24] V. G. Chigrinov, V. M. Kozenkov, H. S. Kwok, *Photoalignment of Liquid Crystalline Materials: Physics and Applications*, John Wiley & Sons, West Sussex, UK **2008**.